THE ASTROPHYSICAL JOURNAL, 488:350–363, 1997 October 10

EXTREMELY METAL-POOR STARS. IV. THE CARBON-RICH OBJECTS

JOHN E. NORRIS
Mount Stromlo and Siding Spring Observatories, The Australian National University, Private Bag, Weston Creek Post Office, ACT 2611, Australia; jen@mso.anu.edu.au

SEAN G. RYAN[1]
Anglo-Australian Observatory, P. O. Box 296, Epping, NSW 2121, Australia; sgr@aaoepp.aao.gov.au

AND

TIMOTHY C. BEERS
Department of Physics and Astronomy, Michigan State University, East Lansing, MI 48824; beers@pa.msu.edu
Received 1997 March 7; accepted 1997 May 22

ABSTRACT

Abundances are presented for some 20 elements in three extremely metal-poor, carbon-rich stars. All have [Fe/H] < -2.5. Based on their high proper motions and spectroscopic gravities two of them have relatively low luminosity: LP 706−7 is on or near the main sequence, while LP 625−44 is a subgiant. The third is the giant CS 22892−052, discovered to be *r*-processes enriched by Sneden et al. (1994). All three stars have large C and N overabundances, and large enhancements of the heavy neutron-capture elements— $\sim$ 1–2 dex.

In contrast to the *r*-process signature observed in CS 22892−052, however, both LP 625−44 and LP 706−7 are clearly *s*-process enriched, suggesting that they may be progenitors of the well-known halo CH giants, the peculiarities of which are believed to result from mass transfer across a binary system containing an asymptotic giant branch star. In both LP 625−44 and LP 706−7 the distribution of *s*-process elements is heavily weighted toward higher atomic number. [hs/ls] $\sim$ 1.5, considerably larger than the values $\lesssim$0.5 found in the *s*-process enhanced near–main-sequence stars of the disk populations. This implies a much higher neutron exposure per seed nucleus in the Population II objects and identifies $^{13}C(\alpha, n)^{16}O$ as the neutron source.

For LP 625−44 radial velocity and Li abundance data are consistent with the binary hypothesis. LP 706−7, however, remains something of an enigma in these respects: it shows no clear evidence for velocity variations, and its Li abundance lies precisely on the Spite Plateau. We estimate that the probability of this occurring in the Ba/CH class of objects is, roughly, $\lesssim$1%.

In metal-poor stars the incidence of carbon enrichment appears to increase toward the lowest metallicities, and below [Fe/H] $= -2.5$ supersolar values of [C/Fe] are not uncommon. Comparison of the available observational material with the Galactic chemical enrichment model of Timmes et al. (1995) shows that the model produces too little carbon. While the difference may result in the sensitivity of carbon production to modeling uncertainties such as the treatment of convection, we also discuss the possible role of a class of carbon producing zero heavy element supernovae and of massive "hypernovae" discussed by Woosley & Weaver (1982, 1995) in explaining this result.

The carbon problem is also implicit in the suggestion that the *r*-process signature seen in CS 22892−052 results from normal supernovae enrichment—where then does its large carbon overabundance originate? The models one might invoke to produce carbon overabundances leave black hole remnants in which the layers containing the seed nuclei for the *r*-process are not available for ejection.

Subject headings: nuclear reactions, nucleosynthesis, abundances — stars: abundances — stars: Population II

1. INTRODUCTION

Among the most metal-deficient stars there appears to be a high incidence of objects with enhanced carbon. In the objective-prism selected catalog of Beers, Preston, & Shectman (1992, hereafter BPS), for example, $\sim$10% of stars with [Fe/H] $\lesssim -2.0$ have stronger than normal *G*-band strengths, as may be seen in Figure 1, which presents the strength of the *G* band as a function of metal abundance. Further, in a search for extremely metal-poor objects among high proper motion stars two of the present authors became intrigued to learn that two of the six stars they found with [Fe/H] < -3.0—the dwarf LP 706−7 and the subgiant LP 625−44 (Ryan & Norris 1991a, 1991b)—have abnormally strong *G* bands. These two objects are shown in Figure 1 as stars. Finally, while only a somewhat limited spectroscopic analysis has yet been presented, we recall also that the claim of the lowest heavy element abundance yet made pertains to the carbon-rich dwarf G77−61, for which Gass, Liebert, & Wehrse (1988) report [Fe/H] $= -5.6$.[2]

At less extreme abundances the proportion of carbon-enhanced objects seems more modest. Consideration of Tables 5 and 8 of BPS reveals that in the ranges

[1] Royal Greenwich Observatory, Madingley Road, Cambridge CB3 0EZ, UK.

[2] We implicitly exclude from our discussion the iron-deficient post–asymptotic giant branch stars discussed by Bond (1992) and Van Winckel, Waelkens, & Waters (1995), for which the iron deficiency is believed to result from fractionation processes rather than being primordial to the stars themselves.

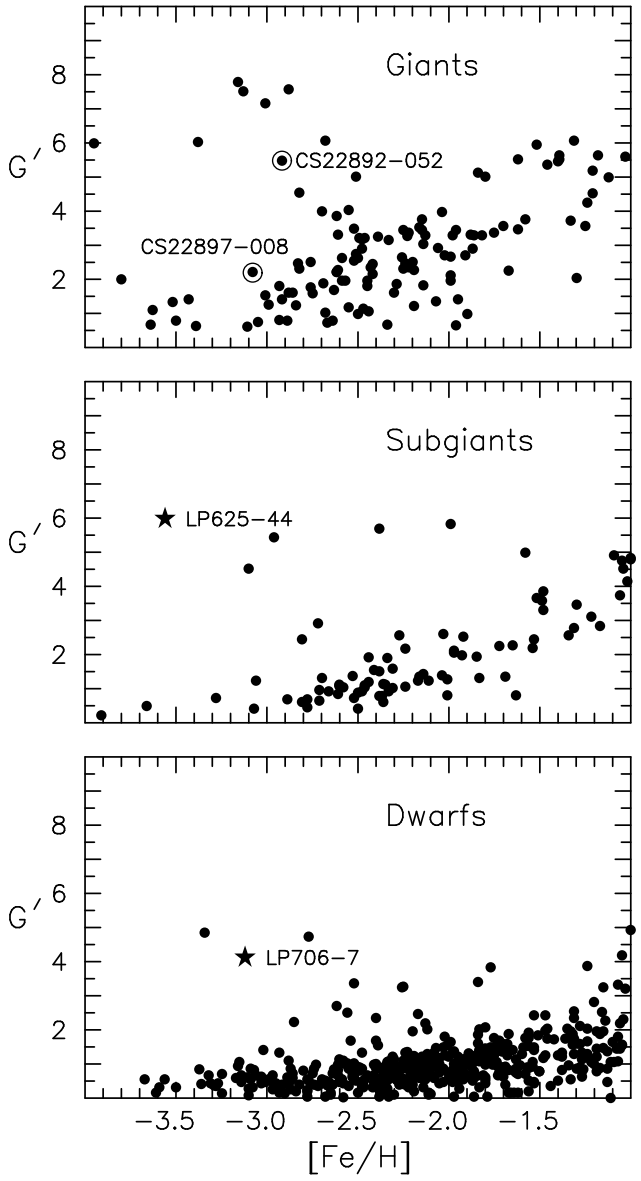

FIG. 1.—*G*-band strength, *G*′, as a function of [Fe/H] for metal-poor stars from BPS (*circles*), and for LP 625−44 and LP 706−7 from spectra obtained by Ryan & Norris (1991a) and Beers, Norris, & Ryan (1997) (*stars*) and the formalism of BPS. (The abundances are based on the Ca II K line on 1 Å resolution spectra, while the luminosity classification is that of BPS, where the giants include their G and AGB classes.)

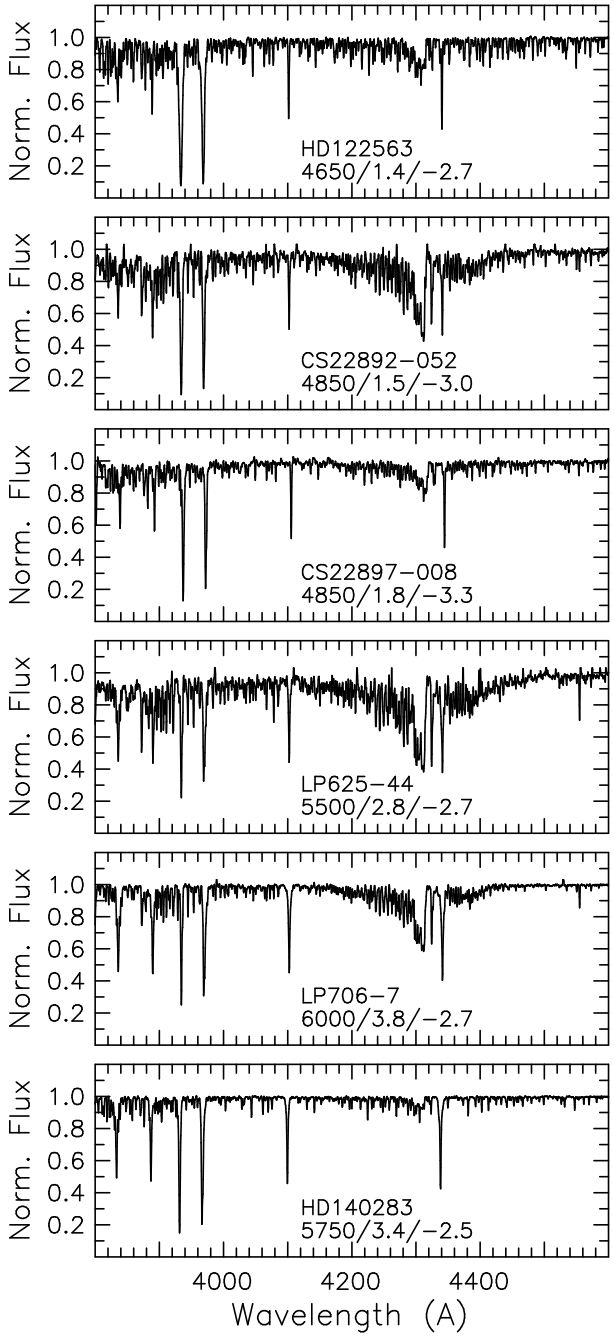

FIG. 2.—Spectra of the carbon-enhanced program stars LP 625−44, LP 706−7, CS 22892−052, and the moderately carbon-rich CS 22897−008, in comparison with the more normal Population II giant HD 122563 and the subgiant HD 140283. Values of $T_{\rm eff}$/log g/[Fe/H], based on the results of Ryan et al. (1996b) and the present work, are also shown.

[Fe/H] < -2.5, $-2.5 <$ [Fe/H] < -1.5, and $-1.5 <$ [Fe/H] < -0.5 the percentages of CH strong objects are 14, 4, and 4, respectively, while Luck & Bond (1991) report that the (disk population) subgiant CH stars, for which their study yields $\langle$[Fe/H]$\rangle = -0.4$, comprise only 1% of stars of similar temperature and gravity. That is to say, the incidence of carbon enhancement appears to decrease with increasing metallicity. It is perhaps also worth noting that the incidence of giant CH stars in halo globular clusters ($\langle$[Fe/H]$\rangle = -1.6$) is low (see McClure 1979), and that in ω Centauri, the only system known to contain more than one of them, the incidence among the brighter giants is $\sim$1% (see Norris & Da Costa 1995, footnote 2).

Canonical wisdom suggests that carbon enhancement in Population II stars results from transfer of carbon across a binary system containing an asymptotic giant branch (AGB) star (see, e.g., McClure, Fletcher, & Nemec 1980), and one might naively argue that the incidence of carbon enhanced objects should increase toward lower abundance since it becomes easier to reverse the carbon/oxygen balance at lowest oxygen abundance. There are two reasons, however, for thinking that this might not necessarily be the full story. The first is that if 14% of the most metal-weak stars are carbon enhanced one has a rather stringent requirement on the fraction of such systems that form in binaries with just the right configuration for the required mass transfer to occur. The second, and somewhat

more compelling argument, is the discovery of Sneden et al. (1994, 1996), that in the carbon-enhanced metal-poor object CS 22892−052, with [Fe/H] = −3.0, the heavy neutron-capture elements are present in *r*-process proportion rather than in an *s*-process one as might be expected from enrichment from an intermediate—mass AGB star. Indeed, Sneden et al. attribute the *r*-process enhancement seen in this star to supernova enrichment of the gas cloud from which it formed. For completeness, the position of CS 22892−052 is also shown in Figure 1.

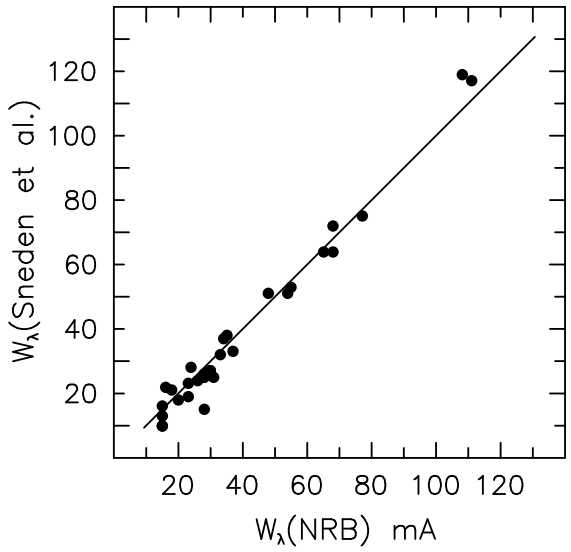

FIG. 3.—Comparison of the equivalent widths presented in Table 1 with those of Sneden et al. (1996).

Inspection of the figure suggests also that there may exist a relatively large dispersion in *G*-band strengths among what one might regard as "normal" stars. To illustrate that at lowest abundance the spread may not be entirely the result of observational error and the range of effective temperature and surface gravity that exist at a given value of [Fe/H], we also label the position of the giant CS 22897−008 in Figure 1. This star sits on what one might regard as the upper envelope of the "normal" giant distribution, and McWilliam et al. (1995a) report that it has [C/Fe] = 0.34, rather high for a Population II giant. We shall return to this topic in §§ 2.1 and 4.2.

As part of our studies of the most metal-deficient stars (Ryan, Norris, & Beers 1996b) we observed the two carbon-strong stars LP 625−44 and LP 706−7 mentioned above, with a view to determining abundances for as many elements as possible to investigate these matters. Since both are high proper motion objects and are therefore objects of relatively low luminosity, we were keen to determine their relationship to the subgiant CH stars (Luck & Bond 1982, 1991). Following the discovery of the remarkable abundance patterns of CS 22892−052 by Sneden et al. (1994) we also included it on our observing program for comparison with the other two objects.

TABLE 1

ATOMIC DATA AND EQUIVALENT WIDTHS (mÅ) FOR PROGRAM STARS

λ (Å)	χ (eV)	log *gf*	LP 625−44	LP 706−7	CS 22892−052	Method
			Li I			
6707.8.....	...	...	<15	31	<15	...
			Sr II			
4077.71.....	0.00	+0.17	...	79	...	W6
4215.52.....	0.00	−0.17	130	68	151	W6
			Y II			
3774.33.....	0.13	+0.21	70	19	78	W6
3788.70.....	0.10	−0.07	79	18	77	W6
3818.34.....	0.13	−0.98	42	<10	35	W6
3950.36.....	0.10	−0.49	56	<10	65	W6
4398.01.....	0.13	−1.00	...	<10	48	W6
5087.43.....	1.08	−0.17	<15	<10	23	W6
5205.73.....	1.03	−0.34	<15	<10	18	W6
			Zr II			
4161.21.....	0.71	−0.72	57	<10	37	W6
4208.99.....	0.71	−0.46	44	<10	34	W6
4496.97.....	0.71	−0.59	29	<10	28	W6
			Ba II			
4554.03.....	0.00	+0.17	281	157	148	syn
5853.69.....	0.60	−1.01	107	37	68	W6
6141.73.....	0.70	−0.07	176	90	108	W6
6496.91.....	0.60	−0.38	159	88	111	W6
			La II			
3988.52.....	0.40	+0.08	117	23	54	syn
3995.75.....	0.17	−0.02	98	22	56	syn
4086.71.....	0.00	−0.16	75	28	62	syn
4123.23.....	0.32	+0.12	85	20	51	syn
4333.76.....	0.17	−0.16	116	...	...	syn

TABLE 1—*Continued*

λ (Å)	χ (eV)	log *gf*	LP 625−44	LP 706−7	CS 22892−052	Method
			Ce II			
4073.47.....	0.48	+0.32	51	<10	15	W6
4083.23.....	0.70	+0.24	56	<10	28	W6
4127.38.....	0.68	+0.24	46	11	...	W6
4222.60.....	0.12	−0.18	52	<10	26	W6
4418.79.....	0.86	+0.31	60	<10	<15	W6
4486.91.....	0.30	−0.36	40	<10	15	W6
4562.37.....	0.48	+0.33	57	8	28	W6
4628.16.....	0.52	+0.26	49	<10	23	W6
			Nd II			
4021.34.....	0.32	−0.17	50	<10	31	W6
4061.09.....	0.47	+0.03	67	20	55	W6
4069.27.....	0.06	−0.40	41	<10	30	W6
4109.46.....	0.32	+0.18	85	16	68	W6
4232.38.....	0.06	−0.35	46	<10	30	W6
4446.39.....	0.20	−0.63	46	<10	28	W6
4462.99.....	0.56	−0.07	52	<10	33	W6
5249.60.....	0.98	+0.08	24	<10	<15	W6
5293.17.....	0.82	−0.20	34	<10	<15	W6
5319.82.....	0.55	−0.35	44	<10	16	W6
			Sm II			
3896.97.....	0.04	−0.58	<15	<10	20	W6
4318.94.....	0.28	−0.27	27	<10	24	W6
4519.63.....	0.54	−0.43	22	<10	15	W6
4537.95.....	0.48	−0.23	21	<10	15	W6
			Eu II			
3819.67.....	0.00	+0.49	bl	bl	bl	syn
4129.70.....	0.00	+0.20	97	<10	132	syn
4205.05.....	0.00	+0.12	bl	<10	bl	syn
4435.56.....	0.21	−0.09	bl	<10	99	syn(bl)[a]
			Dy II			
4077.96.....	0.10	−0.01	bl	...	bl	syn(bl)[a]

[a] Blending features are Sr II 4077.71 and Ca I 4435.69, with log *gf* values of 0.15 and −0.52, respectively.

The present work reports the results of our investigation. Section 2 describes the observational material, while in § 3 we present the chemical abundances that result from analysis of the data. An additional aim of the program was to address the more general question of the spread in [C/Fe] in the most metal-poor stars alluded to above. To this end we have also determined carbon abundances, or limits, for the objects analyzed by Ryan et al. (1996a). In § 4 we discuss the implication of the abundances.

2. OBSERVATIONAL MATERIAL

2.1. *Spectroscopy*

LP 625−44, LP 706−7, and CS 22892−052 were observed with the University College London coudé echelle spectrograph, Anglo-Australian Telescope combination as part of our study of the most metal-poor stars during the period 1992 through 1994, over the wavelength ranges 3720–4670 and 5050–6800 Å.[3] The reduction of the blue data, as part of our larger investigation, is described in detail by Norris, Ryan, & Beers (1996), and we refer the reader to that work for the procedures and line strength measurements. Suffice it here to recall that the spectra were taken with resolving power 40,000, and the net number of detected photons in the co-added spectra were 4300, 3900, and 2500 per 0.04 Å pixel at 4300 Å, respectively. The error of measurement for lines weaker than 60 mÅ, as determined from the repeatability of the same lines measured on contiguous orders, was 4 mÅ in all cases. The same techniques were used to reduce and analyze the red spectra, which had 1800, 1000, and 3700 detected photons per 0.04 Å pixel at 6000 Å, respectively, and from which we sought to measure the strengths of the Li I feature at 6707.8 Å and the lines of heavy neutron-capture elements.

To give the reader a feeling for the nature of the spectra of the program stars, Figure 2 presents a comparison of them

TABLE 2

BROADBAND PHOTOMETRY FOR PROGRAM STARS

Star	*B*−*V*	*R*−*I*	*E*(*B*−*V*)
LP 625−44	0.69	0.42	0.08
LP 706−7.....	0.46	0.305	0.00
CS 22892−052.....	0.78	...	0.02

[3] For LP 706−7 the red data were obtained with incomplete wavelength coverage over the range 5400–6750 Å, during AAT service observations in which a different grating was employed from that used in our other work. We are grateful to Jason Spyromilio for making this observation for us. A spectrum of this star was also obtained over the wavelength range 5340–8170 Å.

with the archetypal metal-poor subgiant HD 140283 and giant HD 122563, which both have [Fe/H] ~ -2.5, in the wavelength range 3800–4600 Å. All of the data in the figure were obtained with the UCL echelle spectrograph employed in the present work, and have been broadened to 1 Å resolution. Note the great strength of the CH absorption at 4300 Å in the program stars, in comparison with that in the more normal Population II objects.

For future reference we include the spectrum of the red giant CS 22897–008 in Figure 2. We highlighted in § 1 that this object, which has [Fe/H] $= -3.2$ and [C/Fe] $= 0.34$, lies on the upper envelope of normal giants in the (G', [Fe/H]) plane.

To supplement the line strengths measures of Norris et al. (1996) with data for the neutron-capture elements (which are in most cases not detected in stars of normal Population II abundance) we attempted to measure lines from the comprehensive list given in Table 1 of Sneden et al. (1996). Our line strengths, together with excitation potentials and log gf values from Sneden et al., as well as results for Li I 6707.8 Å, are presented in Table 1. The reader will find that not all lines from Table 1 of Sneden et al. are included in the table. An atomic species was generally included only if in our spectra (which have somewhat lower signal-to-noise than those of Sneden et al., but twice the resolution) two or more lines could be well measured. Further, in some cases we rejected a line of a species included in their Table 1 if we came to the view that blending compromised our ability to determine an accurate abundance.

A detailed comparison of line strengths measured in our investigations of metal-poor stars with those of other workers has been given in Norris et al. (1996, Figs. 3–6), to which we refer the reader. In Figure 3 we compare the data in Table 1 with those of Sneden et al. (1996) for CS 22892−052, where one sees excellent agreement between the two data sets. Our measurements of the strength of Li I 6707.8 Å in LP 625−44 and LP 706−7 agree well with those of Thorburn (1994)—we find 31 and less than 15 mÅ, respectively, while she reports 27 and less than 3 mÅ.

2.2. *Broadband Photometry*

Photoelectric $BVRI$ values for the program stars, based on Ryan (1989), BPS, and Norris, Ryan, & Beers (1997) are presented in Table 2, together with the reddening values based on those works. These data will provide the basis for the effective temperatures utilized in the following section.

3. CHEMICAL ABUNDANCES

We have used the model atmosphere techniques described in considerable detail by Ryan et al. (1996b) in their analysis of some 19 of the most metal-poor stars to determine abundances for elements in the range Mg–Dy, and refer the reader to that work for details of the process and the sources of the adopted gf values, and to Sneden et al. (1996) for the treatment of the heaviest elements. In the present investigation we have also employed spectrum synthesis techniques using the code of Cottrell (see Cottrell & Norris 1978) to estimate abundances for C and N, and for those neutron-capture elements for which hyperfine structure (hfs) is important. We note explicitly that in the present work as in that of Ryan et al. we employ the model atmospheres of Bell et al. (1976) and Bell (1983). In what follows we shall concentrate only on details that are most pertinent to the present investigation, and refer the reader to Ryan et al. for other details.

3.1. *Atmospheric Parameters*

Effective temperatures for the three program stars, based on the observed $R-I$ and $B-V$ photometry, the reddenings from § 2.2, and the procedure of Ryan et al. (1996b) are presented in the first row of Table 3. Given the CH line enhancement in the B band, which might affect $B-V$, we decided to give precedence to $R-I$. Thus, for LP 625−44 and LP 706−7 the effective temperatures are derived from $R-I$ alone. For these two objects the $R-I$ based temperatures are hotter, on average, by 250 K than those determined from $B-V$. When we undertook our analysis, $R-I$ was not available for CS 22892−052, and the adopted temperature is derived from the observed $B-V$ value. (Subsequently, we measured $R-I = 0.501$, which yields $T_{\rm eff} = 4950$ K, in good agreement with the value presented in Table 3.) Initially, surface gravities of log $g = 4.5$, 4.5, and 2.0 were assumed for LP 625−44, LP 706−7, and CS 22892−052, respectively, based on our perception of their evolutionary status, and these were revised to obtain a satisfactory ionization balance between Fe I and Fe II lines for the latter of which two, two, and eight lines were available, respectively. The final adopted gravities, microturbulences ξ determined from Fe I lines, and values of [Fe/H] are presented in the second, third, and fourth rows of the table. Similar data for the metal-poor red giant HD 122563 from Ryan et al. (1996b), supplemented by abundances from Sneden & Parthasarathy (1983) for elements heavier than Ba, are also presented in the table for later comparison purposes.

The atmospheric parameters for LP 625−44 and LP 706−7 are those appropriate to a subgiant near the base of the giant branch and a near–main-sequence object, respectively. The proper motions of these objects place stringent restrictions on their absolute magnitudes, and confirm these designations. LP 625−44 has (V, μ) = (11.85, 0.″20 yr^{-1}) (Ryan & Norris 1991a), and if it were brighter than $M_V = 2.5$, its tangential velocity would be greater than 700 km s^{-1}. Similarly, LP 706−7 has (V, μ) = (12.11, 0.″31 yr^{-1}): For $M_V < 4.0$, its tangential velocity would exceed 600 km s^{-1}.

3.2. *Carbon and Nitrogen*

Carbon and nitrogen abundances have been determined by fitting the features of CH at 4323 Å and CN at 3883 Å to model atmosphere synthetic spectra. In all cases we adopted [O/Fe] = 0.6, typical of Population II material, since we have not detected oxygen in our program stars. (We place an upper limit of 15 mÅ on the strength of the O I 6300.3 Å line in LP 625−44 and CS 22892−052, and the O I 7771.9 Å feature in LP 706−7. This places no useful limit on oxygen abundances: In LP 706−7, for example, we find [O/Fe] < 1.1, and even larger values for the other stars). Tests on the range $0.0 <$ [O/Fe] < 0.6, however, show that for such C-rich objects the abundances are insensitive to the assumption. Our procedure is similar to that described in Norris & Da Costa (1995), where difficulties were encountered in fitting the violet CN band of HD 122563. In the present work we have adopted a dissociation energy of the CN molecule of 7.66 eV (see Lambert 1978) and adjusted the normalization of the oscillator strengths to obtain a fit

TABLE 3

ATMOSPHERIC PARAMETERS AND ABUNDANCES FOR PROGRAM STARS[a]

		LP 625−44			LP 706−7			CS 22892−052			HD 122563		
PARAMETER/ABUNDANCE	ION	Ab	se	*n*	Ab	se	*n*	Ab	se	*n*	Ab	se	*n*
$T_{\rm eff}$ (K)			5500			6000			4850			4650	
log *g* (cgs)			2.8			3.8			1.5			1.4	
ξ (km s^{-1})			1.0			1.3			2.5			2.6	
[Fe/H]	Fe I	−2.68	0.31	47	−2.74	0.16	74	−2.97	0.20	100	−2.68	0.11	165
[C/Fe]	CH	+1.95	0.22	...	+2.15	0.23	...	+1.10	0.23	...	−0.45	0.20	...
[N/Fe]	CH,CN	+1.65	0.44	...	+1.80	0.35	...	+1.00	0.42	...	+1.00[b]	...	...
[Mg/Fe]	Mg I	+0.82	0.20	4	+0.45	0.11	3	+0.42	0.12	4	+0.32	0.04	7
[Al/Fe]	Al I	−0.24	0.10	1	−0.67	0.11	1	−0.54	0.15	1	−0.24	0.10	1
[Ca/Fe]	Ca I	+0.61	0.20	4	+0.39	0.09	5	+0.33	0.11	6	+0.14	0.06	9
[Sc/Fe]	Sc II	+1.13	0.12	1	−0.16	0.18	1	−0.20	0.18	3	+0.25	0.11	7
[Ti/Fe]	Ti I	+0.98	0.55	2	+0.41	0.15	2	+0.19	0.26	3	+0.12	0.05	10
[Ti/Fe]	Ti II	+0.45	0.20	10	+0.17	0.15	13	+0.25	0.16	25	+0.34	0.08	32
[Cr/Fe]	Cr I	−0.02	0.16	1	−0.04	0.17	2	−0.74	0.10	1	−0.39	0.07	7
[Mn/Fe]	Mn I	−0.68	0.11	2	−0.63	0.11	2	−0.81	0.09	2	−0.37	0.05	5
[Co/Fe]	Co I	−0.04	0.21	1	+0.14	0.34	2	+0.29	0.10	4	+0.33	0.07	5
[Ni/Fe]	Ni I	+0.72	0.47	2	−0.11	0.08	4	+0.20	0.18	5	+0.21	0.08	9
[Sr/Fe]	Sr II	+0.73	0.13	1	+0.15	0.18	2	+0.17	0.29	1	−0.21	0.10	2
[Y/Fe]	Y II	+1.38	0.23	4	+0.25	0.19	2	+0.28	0.18	7	−0.16	0.18	1
[Zr/Fe]	Zr II	+1.62	0.36	3	< +1.16	0.21	1	+0.59	0.24	3	−0.10	0.22	1
[Ba/Fe]	Ba II	+2.57	0.17	4	+2.01	0.14	4	+0.55	0.20	4	−0.84	0.10	1
[La/Fe]	La II	+2.56	0.24	5	+1.81	0.19	4	+0.96	0.22	4	−0.67[c]	...	...
[Ce/Fe]	Ce II	+2.70	0.22	8	+1.86	0.31	2	+1.00	0.23	6	< −0.32[c]	...	...
[Nd/Fe]	Nd II	+2.61	0.21	10	+2.01	0.27	2	+1.25	0.21	8	−0.52[c]	...	...
[Sm/Fe]	Sm II	+2.19	0.26	3	< +2.21	0.20	1	+1.35	0.24	4	< −0.52[c]	...	...
[Eu/Fe]	Eu II	+1.75	0.31	4	+1.40	0.20	1	+1.52	0.19	4	−0.32[c]	...	...
[Dy/Fe]	Dy II	+1.70	0.17	1	...	...	...	+1.30	0.21	1	−0.32[c]	...	...

[a] For each star the three columns give abundance, standard error, and number of lines.
[b] By definition. See § 3.2.
[c] From Sneden & Parthasarathy (1983), assuming [Fe/H] = −2.68.

to the observed spectrum of HD 122563 for [N/Fe] = 1.0, based on the values of 1.2 and 0.6 obtained from the NH bands in this star by Sneden (1973) and Carbon et al. (1982), respectively. The comparison of the observational data for the three carbon-rich objects and HD 122563 with the computations is shown in Figure 4, while the resulting abundances are given in Table 3. We note that our value of [C/Fe] = −0.45 for HD 122563 is in good agreement with that of −0.4 of Sneden (1973), while our result of ([C/Fe], [N/Fe]) = (1.1, 1.0) for CS 22892−052 compares well with (1.1, 0.8) reported by Sneden et al. (1996, Fig. 6).

3.3. *Heavier Elements*

Abundances, [M/Fe], for 19 heavier elements, their errors, and the number of lines utilized in the determination are presented in Table 3.

3.3.1. *Elements Unaffected by Hyperfine Structure*

For most elements hyperfine structure is unimportant, and in these cases abundances were determined by using the code WIDTH6 as described by Ryan et al. (1996b). This is the case for all elements less massive that Ni in the present investigation, with the exceptions of Mn and Co. For the latter cases we follow Ryan et al., who used spectrum synthesis computations to determine corrections necessary to modify the WIDTH6 derived abundances.

3.3.2. *Elements Affected by Hyperfine Structure and Blending*

For several of the heavy neutron-capture elements hyperfine structure plays an important role in broadening of spectral lines and must be accounted for in the analysis. For transitions affected by hfs we used spectrum synthesis to determine abundances on a line-by-line basis. Spectrum synthesis also permits one to investigate lines that are moderately blended with other features. As noted in § 2.1 we were guided in our choice of transitions of the neutron-capture elements by the work of Sneden et al. (1996). In the final column of Table 1 we indicate whether we treated the line by using WIDTH6 (W6), by spectrum synthesis (syn), or by spectrum synthesis that includes the effect of blending with another feature (syn(bl)).

At some level, hyperfine structure splitting affects most odd atomic mass elements. In practice, however, only in a few transitions does the splitting and line strength distribution result in changes to the curve of growth by more than 0.01 dex or so. As a rough guide, level splittings for a given isotope are generally larger for lower excitation energies, with the result that resonance lines tend to exhibit greater hfs broadening than those associated with excited levels. Isotope shifts are generally smaller in magnitude. In the present investigation hfs is important for Ba, La, and Eu, and we have explicitly included its effects following McWilliam et al. (1995a), Sneden et al. (1996), and White & Eliason (1933).

Barium has five main isotopes, three of which have even masses (and hence no hyperfine splitting) and negligible isotope shifts. Although we computed the contribution of each hfs component in our analysis, utilizing the level splittings tabulated by Rutten (1978, Table II), it helps to think of the composite line as comprising just three components: a central line due to the even isotopes, plus a blue- and a redshifted line due to the odd isotopes (e.g., Rutten 1978, Table I). As set out by Sneden et al. (1996), the *s*-process produces all five isotopes, but only 11% of the total is due to the odd isotopes. The *r*-process, at the other extreme, gener-

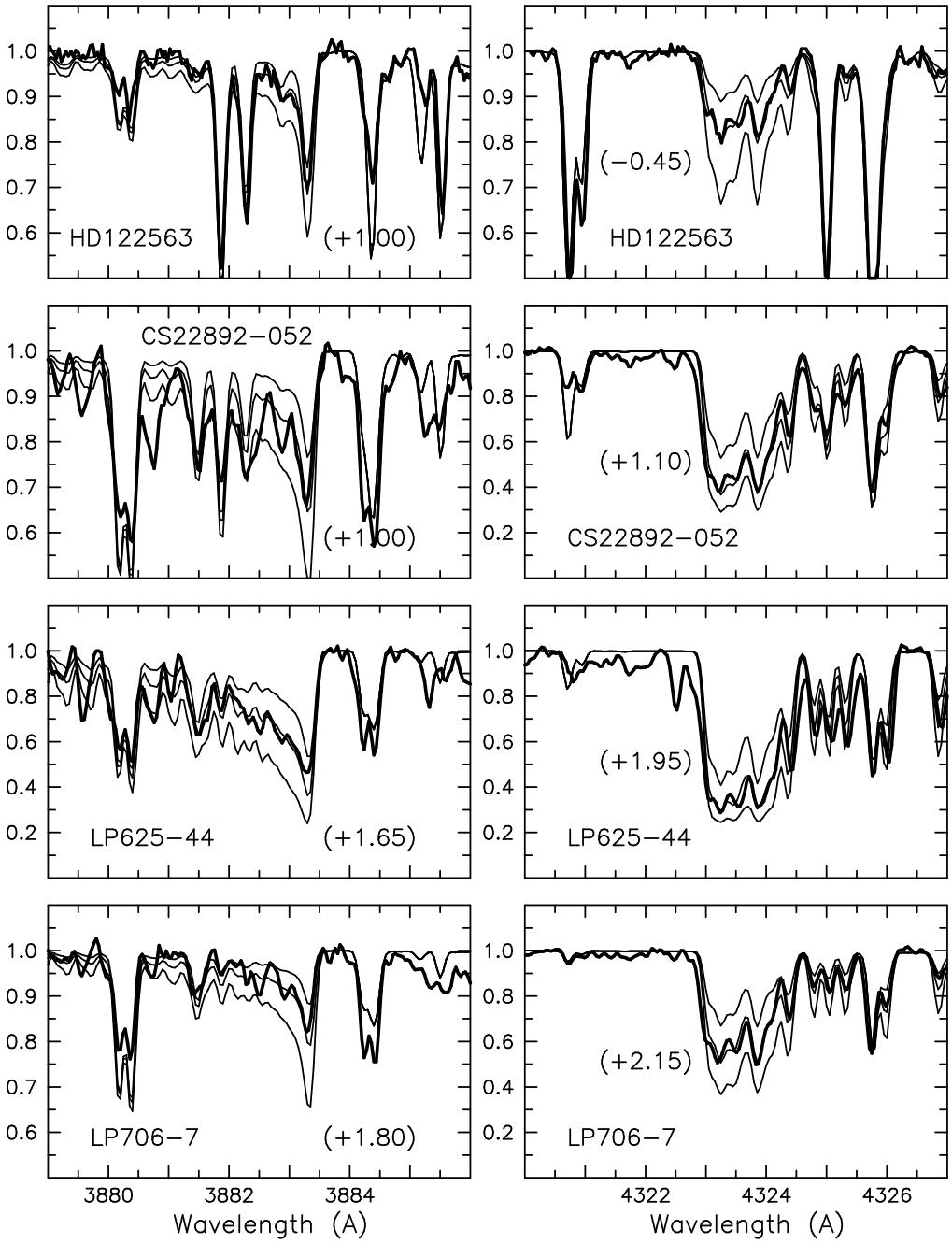

FIG. 4.—Comparison of the observed spectra (*thick lines*) with synthetic spectra (*thin lines*) in the region of violet CN at 3883 Å and CH at 4323 Å. On the right the three synthetic spectra differ in steps of Δ[C/Fe] = 0.3, while on the left the computations were done with the best-fit [C/Fe] determined at 4323 Å and steps of Δ[N/Fe] = 0.3. The adopted values of [C/Fe] and [N/Fe] are given in parentheses in the right and left panels, respectively. (The ordinate is relative intensity.)

ates 52% of its yield as odd isotopes. Thus, the magnitude of the hyperfine structure correction for this element depends on the origin of the material being studied. We used a line list with three different *gf* tabulations appropriate to pure *s*-process, pure *r*-process, and solar system material (a hybrid between the two, but essentially *s*-process–like) and computed hfs corrections for each isotope mixture. Only for Ba II 4554 Å was the effect important.

One coarse estimate of the importance of hfs may be made from the overall line splitting within a transition, though clearly the distribution of line strengths within the profile is also very important. The overall splitting of Ba II 4554 Å is 58 mÅ but is only 24 mÅ in Ba II 6496 Å for which hfs was found to be insignificant ($\leq$0.02 dex in our stars).

Lanthanum has only a single significant isotope, but generally large hyperfine splitting in the lower levels (Höhle, Hühnermann, & Wagner 1982). For most of the transitions we studied, the upper level splittings were unknown to us, so on the grounds that level splittings are *generally* much lower for higher excitation levels, we treated these as zero. Significant line splittings emerged for all except La II 4123 Å, ranging in the other lines from 36 to 137 mÅ.

The remaining element for which hfs was large is Eu, for which we adopted equal contributions of the two isotopes.

The splittings, computed using the interaction coefficients of Krebs & Winkler (1960), ranged from 160 to 240 mÅ.

3.3.3. *Error Estimates*

The errors for the three program stars in Table 3 were estimated following the treatment of Ryan et al. (1996b), to which we refer the reader for details. Suffice it here to say that the values were obtained by adding in quadrature the individual errors corresponding to uncertainties of $\Delta T_{\rm eff} =$ 170, 100, and 100 K for LP 625−44, LP 706−7, and CS 22892−052, respectively, $\Delta \log g = 0.3$ dex and $\Delta\xi = 0.5$ km s^{-1} for all stars, and the random error in the abundance of the element resulting from errors of line measurement and *gf* values. For the latter component we adopted max (0.10/$n^{1/2}$, s.e.), where s.e. is the standard error obtained from n lines. Finally, for carbon and nitrogen we adopt a fitting error of 0.1 dex as the random observational error, and for nitrogen we also propagate in quadrature the observational error in the carbon abundance.

4. DISCUSSION

4.1. *Overall Abundance Patterns*

Figure 5 presents [M/H] as a function of atomic number for the three program stars and the normal Population II object HD 122563, where the horizontal lines pass through the values of [Fe/H]. All four objects have the same value of [Fe/H] to within ∼0.3 dex, which facilitates direct comparison. The outstanding features of the three carbon enriched stars are their huge enhancements of C, N, and neutron-capture elements beginning at Ba. Large overabundances are also evident for the neutron-capture elements Sr, Y, and Zr in LP 625−44, while smaller ones appear to be present for LP 706−7 and CS 22892−052.

Inspection of the figure reveals differences between the heavy neutron-capture element patterns of CS 22892−052 on the one hand, and LP 625−44 and LP 706−7 on the other. In particular the *s*-process/*r*-process indicator [Ba/Eu] is quite different: [Ba/Eu] = −0.97 ± 0.20 for CS 22892−052, and +0.82 ± 0.23 and +0.61 ± 0.31 for LP 706−7 and LP 625−44, respectively. We defer discussion of this point to § 4.3.

The only other striking feature of Figure 5 is the large overabundance of Sc, ∼0.9 dex, in LP 625−44 relative to HD 122563. Given, however, that this is based on only one line (albeit relatively strong with $W_\lambda = 114$ mÅ), we are reluctant to overemphasize the enhancement and will not discuss it further here, except to make two points. First, the effect is much larger than may be understood in term of reasonable errors in $T_{\rm eff}$, log g, [Fe/H], and ξ, or (as far as we can determine) blending with features of the CH molecule. Second, while we have not included hyperfine structure in our treatment of Sc, even though it has odd-numbered atomic mass, inspection of Table 6 of McWilliam et al. (1995a) shows that this is a reasonable assumption, leading to errors less than 0.05 dex for a line of the strength under discussion here. Possible small enhancements of ∼0.4 dex for Cr may also be present in LP 625−44 and LP 706−7, but here too the evidence is not compelling.

4.2. *Carbon*

In Figure 6 we show [C/Fe] as a function of [Fe/H] for the C-strong stars of the present investigation and the giants of Ryan et al. (1996b), together with other recent data

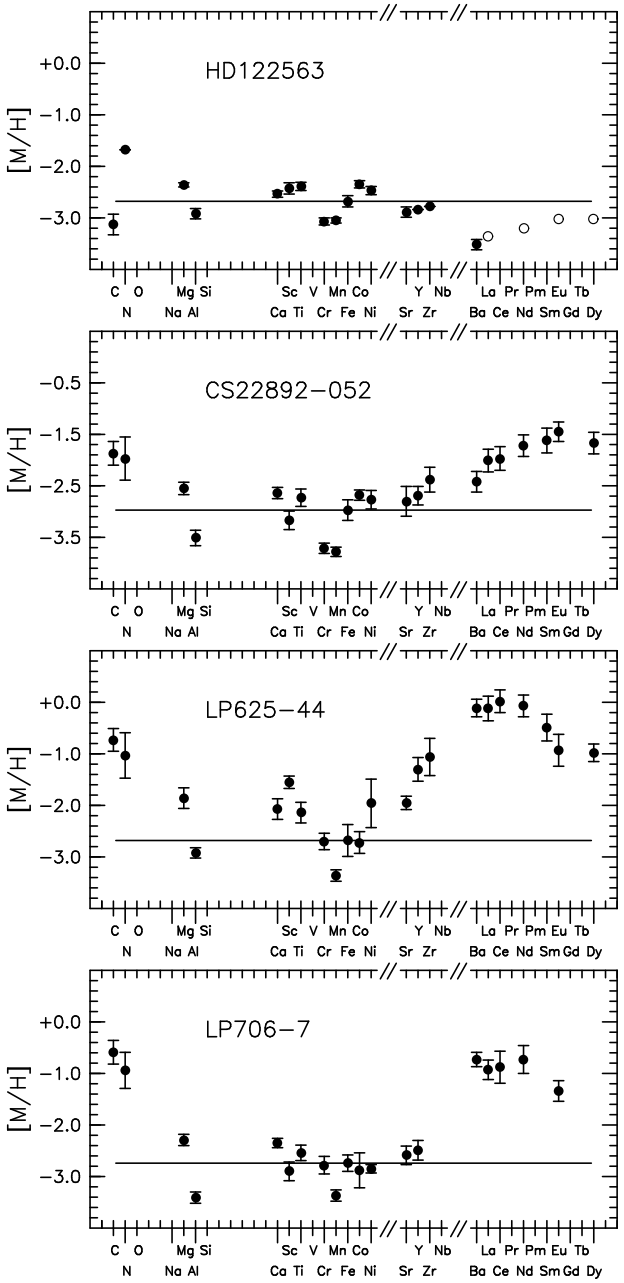

FIG. 5.—[M/H] as a function of atomic species for the program stars and HD 122563. Filled and open symbols represent data from the present work and Sneden & Parthasarathy (1983), respectively. The horizontal lines pass through the data for [Fe/H].

from the literature. (Table 4 presents values of [C/Fe], or limits, determined from the spectra presented in Norris et al. (1996) and the techniques described in our § 3.2.) Stars observed by more than one set of authors are connected, and provide an external error estimate. Predictions of the Galactic chemical enrichment model of Timmes, Woosley, & Weaver (1995, their Fig. 13) are also shown.

One obtains the impression from Figure 6 that at the lowest abundances C has been overproduced in a large fraction of objects. Wheeler, Sneden, & Truran (1989) show a similar trend on the range −2.5 < [Fe/H] < −1.5. Below [Fe/H] = −2.5 in Figure 6, the effect is seen not only for abundances in the present work and that of Ryan, Norris, & Bessell (1991) (*filled and open stars*), which involve both

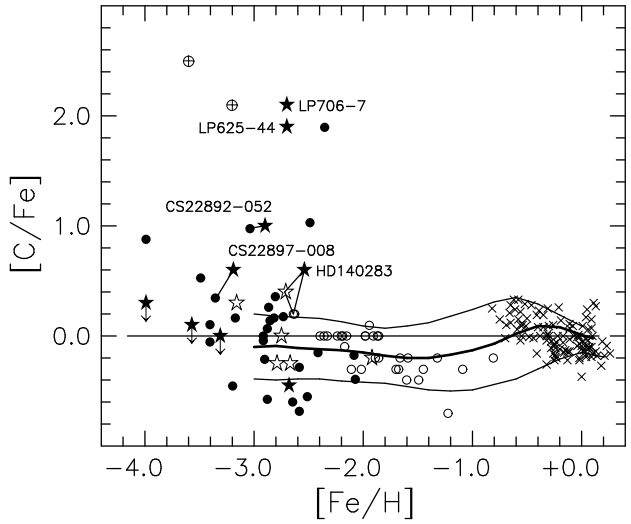

FIG. 6.—[C/Fe] vs. [Fe/H] for metal-deficient stars. Filled and open stars come from the present work and Ryan et al. (1991), respectively; filled circles from McWilliam et al. (1995a, excluding values designated uncertain); crossed circles from Barbuy et al. (1996); and open circles and crosses are from Tomkin et al. (1992, 1995), respectively. The thick line represents the result of the chemical enrichment model of Timmes et al. (1995), while the thin lines show the effect of increasing and decreasing the model Fe production by a factor of 2.

dwarfs and giants, but also in that of McWilliam et al. (1995a) (*filled circles*), which includes only giants and subgiants. Given that carbon depletions are often seen in metal-poor field and globular cluster red giants (see, e.g., Carbon et al. 1982; Kraft et al. 1982; Langer et al. 1986)—an effect most readily understood in terms of mixing effects in the stars themselves—the *initial* carbon enhancement may well have been larger than suggested by the figure.

In §§ 1 and 2 we commented on the C enhancement of CS 22897−008, which appeared to lie on the upper envelope of what one might regard as "normal" stars in the (G', [Fe/H]) plane. Its position is also shown in Figure 6, where one sees that it is indeed carbon enhanced, with [C/Fe] $\sim$ 0.5, based on the analysis of McWilliam et al. (1995a) and the present work.

As emphasized by Gibson (1995, 1997) different model builders sometimes produce different yields for the same input parameters. While comparison is given here with Timmes et al., one should bear in mind that comparison of the data with the predictions of other workers might give somewhat different results. In the present context it is worth noting that the production of carbon is quite sensitive to the treatment of convection.

This having been said, it is interesting to note that in the supernova simulations of some of the 18, 20, 25, and 30 $M_\odot$ zero heavy element objects of Woosley & Weaver (1995), little or no Fe and O but large amounts of C are produced (in contradistinction to the large C/O ratios normally predicted). The salient point is that not all of the outer layers are ejected and much material, in particular the oxygen-rich and ^{56}Ni-rich regions, falls back onto the star. Perhaps it is such objects that lead to an overproduction of carbon.

TABLE 4

CARBON ABUNDANCES FOR METAL-POOR STARS FROM RYAN ET AL. (1996a)

Star	$T_{\rm eff}$	log g	[Fe/H]	[C/Fe]
HD 140283	5750	3.4	−2.54	0.6
CS 22897−008.....	4850	1.8	−3.19	0.6
CD−38°245.....	4850	1.5	−3.96	$\leq$0.3
CS 22172−002.....	4900	1.8	−3.57	$\leq$0.1
CS 22952−015.....	4850	1.6	−3.31	$\leq$0.0

The distribution of [C/Fe] at low abundance is also intriguing. It will be interesting to see if the large gap of almost 1 dex in [C/Fe] between the five stars at [C/Fe] $\sim$ 2 and the remainder of the sample survives observation of further C-rich objects. We note too that the crossed circles in the figure are the CH giants of Barbuy et al. (1997). These have about the same carbon abundance as the near–main-sequence objects LP 625−44 and LP 706−7, which is mildly surprising. If LP 625−44 and LP 706−7 are the progenitors of CH stars, (as we will argue below may be the case) one might expect them, when they evolve up the giant branch, to experience significant dilution of their surface abundance anomalies as their convective envelopes deepen into regions original to the star. On the other hand, the CH giants with [C/Fe] $\sim$ 2 have already experienced this putative dilution and one might ask why we have not observed dwarfs with larger carbon abundances in our surveys for metal-poor stars. The answer may well be that such objects would be blitzed with lines of molecules involving carbon and not appear metal-weak. Indeed, G77−61, which Gass et al. (1988) report to have [Fe/H] = −5.6 and [C/Fe] = 4.2, may be such an object.

4.3. *Heavy Neutron-capture Elements*

A comparison of the heavy neutron-capture element abundances, log ϵ (= log [N(M)/N(H)] + 12), as a function of atomic species is presented in Figure 7 for the three carbon-enriched objects. Also shown for comparison as thin and thick lines are the abundance patterns for typical *r*-process and *s*-process production, respectively. For the former the data were taken from Cowan, Cameron, & Truran (1982), while the latter pertain to the distribution presented by Malaney (1987) for an AGB star of core mass 0.60 $M_\odot$. The fundamental difference between CS 22892−052 on the one hand, and LP 625−44 and LP 706−7 on the other, already alluded to in § 4.1, is clear—the former, as first reported by Sneden et al. (1994), has an *r*-process signature, while the latter are *s*-process enhanced. (We note for completeness here that the Ba abundances in Table 3 assume that Ba II 4554 Å has *s*-process isotopic abundances for LP 625−44 and LP 706−7 on the one hand, and *r*-process ones for CS 22892−052 on the other).

We refer the reader to Sneden et al. (1996) for a thorough discussion of CS 22892−052. The simplest explanation of LP 706−7 and LP 625−44 is that they are main-sequence turnoff and subgiant progenitors of the classical halo CH giant stars, which are also C and heavy neutron-capture element enhanced in an *s*-process distribution (Lambert 1985, and references therein). The disk population counterpart of this relationship is provided by the subgiant CH stars and the Ba II giants (Smith, Coleman, & Lambert 1993, and references therein). In these objects the abundance patterns are generally explained in terms of earlier mass transfer across a binary system containing an AGB star (see, e.g., McClure et al. 1980). We now examine aspects of this possibility in closer detail.

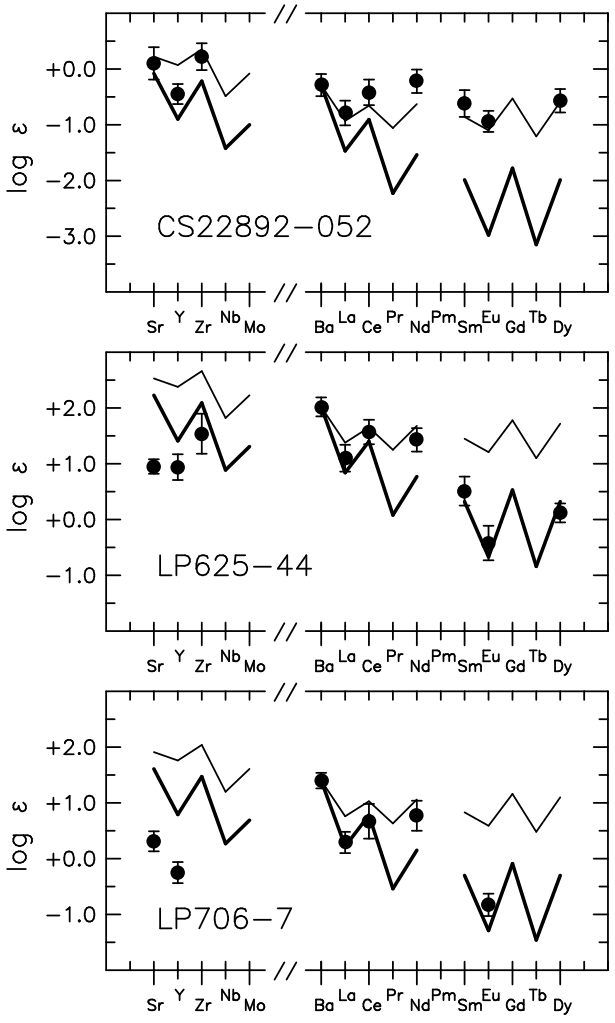

FIG. 7.—Dependence of abundance on atomic species for the heavy neutron-capture elements. The thin and thick lines refer to *r*- and *s*-process distributions from the work of Cowan et al. (1982) and Malaney (1987), respectively. Theory and observation have been normalized at Ba.

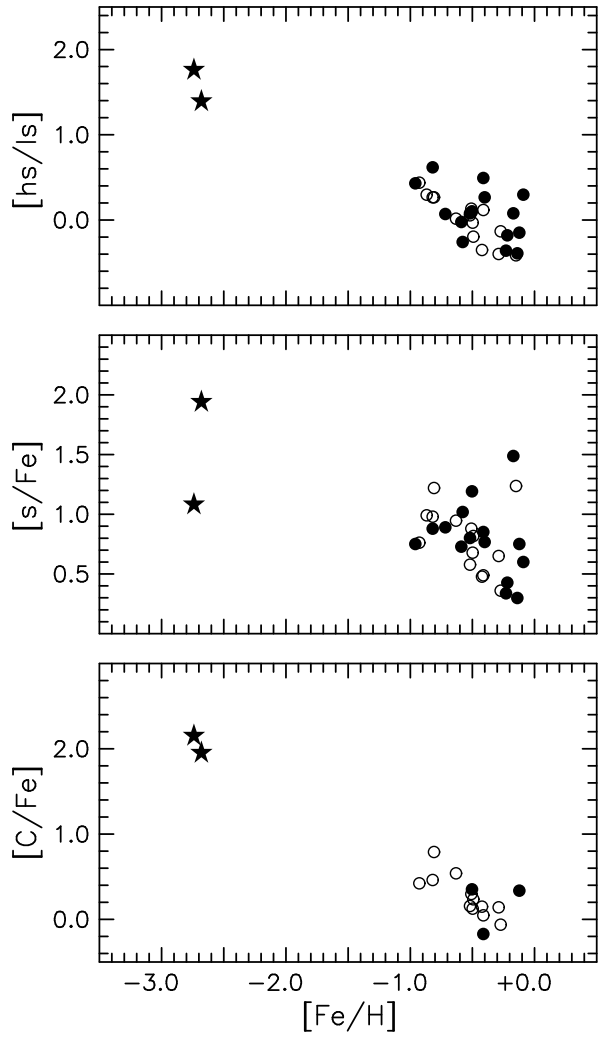

FIG. 8.—[hs/ls], [s/Fe], and [C/Fe] as functions of [Fe/H] for LP 625−44 and LP 706−7 (*stars*), subgiant CH stars (*filled circles*), and the F str λ4077 stars (*open circles*).

4.4. *Comparison with s-process Enhanced Disk Stars*

Figure 8 presents a comparison of our abundance results for LP 625−44 and LP 706−7 with those of the *s*-process–enhanced subgiant CH stars (Luck & Bond 1982, 1991) and F str λ4077 stars (North, Berthet, & Lanz 1994) of the disk populations. The disk objects have gravities that place them on or near the main sequence and make them, at least in the case of LP 706−7, appropriate reference objects. The abundance parameters of the neutron-capture elements follow North et al. The quantity [hs/ls] is defined as the difference between the mean abundance, [hs/Fe], of the heavy *s*-process elements Ba, Ce, and Nd and the mean value, [ls/Fe], of the lighter ones Sr, Y, and Zr. [s/Fe] is the arithmetic mean of [hs/Fe] and [ls/Fe].

It is immediately apparent that LP 625−44 and LP 706−7 are much more extreme in their enhancement of both C and the *s*-process elements than are the disk objects. This is in keeping with the naive expectation that larger pollution effects will be found in metal-poorer environments. What is also apparent from the figure is that the neutron exposure per seed nucleus was also greater at lower metallicity. As discussed by Luck & Bond (1991, § 8), [hs/ls] is a good estimator of the neutron exposure in the *s*-process, being well correlated with the neutron-exposure parameter τ_0 discussed by Cowley & Downs (1980).[4] The strong anticorrelation between [hs/ls] and [Fe/H] is most readily understood in terms of the neutron source being the (primary) $^{13}C(\alpha, n)^{16}O$ reaction rather than the (secondary) $^{22}Ne(\alpha, n)^{25}Mg$ one, as discussed by Luck & Bond and North et al.

4.5. *A Search for Radial-velocity Variations*

Given that the CH giants and subgiants show small, long-period radial-velocity variations (McClure & Woodsworth 1990; McClure 1997) we sought to determine whether similar effects are evident for LP 625−44 and LP 706−7. For this purpose the data described in § 2 were

[4] We sought to compute τ_0 using the procedure of Tomkin & Lambert (1983) and the data of Cowley & Downs (1980). Considerably larger exposures are required for LP 625−44 and LP 706−7 than are admitted by the calculations of Cowley & Downs, which, it may be recalled, were tailored for the more moderate *s*-process enhancements found in disk objects.

supplemented by additional material from the AAT archives, AAT service observing, and our ongoing program with that telescope, together with wavelength-calibrated spectra kindly made available by J. A. Thorburn and described elsewhere (Thorburn 1994). In all but one case the data were obtained with echelle spectrographs. These spectra were wavelength calibrated and velocities were determined from them by direct measurement of the positions of a set of relatively strong, unblended lines that form a subset of those used in our abundance analysis. In the case of the earliest spectrum for LP 625−44, this procedure was complemented with Fourier cross-correlation techniques available in the IRAF package. The two methods gave consistent results. Radial velocities and associated data are presented in Table 5, where the column headings should be self-explanatory, except for column (5), which presents the *internal* standard error of measurement. Since the data were not taken for the determination of accurate radial velocities and come from a number of different telescope/spectrograph/detector combinations, the external measurement error will probably be larger than these values. For the AAT/UCLES/CCD combination used in the present series of papers Norris et al. (1996) set an upper limit to the external standard error of 1.0 km s^{-1}. For completeness we also include data for CS 22892−052 in the table.

Radial velocities are plotted as a function of Julian Day number in Figure 9, which contains the essential results. For LP 625−44 the data, which span some 3000 days, are not inconsistent with a small variation of the kind reported by McClure & Woodsworth (1990), and McClure (1997) for the CH giants. The figure suggests that we have been unfortunate in the interval over which we have been able to observe this object, since its velocity remained relatively constant throughout the echelle observations. We have, however, no reason to doubt the integrity of our earliest, and least well-determined, velocity obtained with the AAT/RGO spectrograph combination on which the case for variability absolutely depends. A period of $\gtrsim$4000 days is not inconsistent with the data.

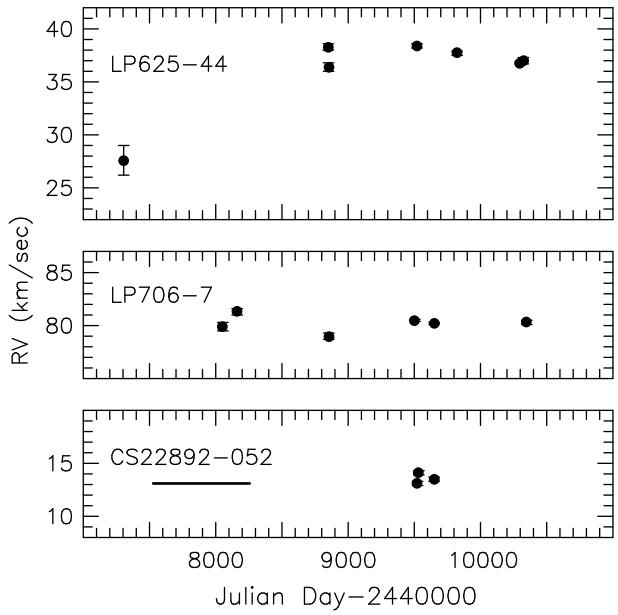

FIG. 9.—Radial velocity as a function of Julian Day number for LP 625−44, LP 706−7, and CS 22892−052. The horizontal line for CS 22892−052 represents the data of McWilliam et al. (1995b).

For LP 706−7 the data span 2300 days. There is no strong evidence for variability, and a determination of the velocity dispersion, using weights inversely proportional to the square of the error of the individual measures, yields a value of 0.4 km s^{-1}. One is hard pressed to make a case for variability of this object from the present data set. We note, however, that the range in values is 2.3 km s^{-1}, which is several times larger than the internal errors presented in Table 5. Given that we are unable to provide a reliable estimate of the external accuracy of measurement, further work is necessary before any statement may be made concerning the reality or otherwise of the range of values seen in the table.

TABLE 5

RADIAL VELOCITIES FOR PROGRAM STARS

Star (1)	UT Date (2)	Julian Day (3)	RV (km s^{-1}) (4)	s.e. (km s^{-1}) (5)	n[a] (6)	Source (7)
LP 625−44	1988 May 23	2447305.10	27.6	1.4	...[b]	AAT/RGO Spect./IPCS[c]
	1992 Aug 16	2448850.93	38.3	0.3	35	AAT/UCLES/CCD
	1992 Aug 18	2448852.52	36.4	0.4	25	Thorburn
	1994 Jun 16	2449520.02	38.4	0.2	37	AAT/UCLES/CCD
	1995 Apr 15	2449823.29	37.7	0.2	19	AAT/UCLES/CCD
	1996 Aug 05	2450299.92	36.8	0.1	46	AAT/UCLES/CCD
	1996 Aug 28	2450322.93	37.0	0.3	10	AAT/UCLES/CCD
LP 706−7	1990 Jun 11	2448054.24	79.9	0.4	14	AAT/UCLES/IPCS[c]
	1990 Sep 27	2448162.19	81.3	0.3	15	AAT/UCLES/IPCS[c]
	1992 Aug 20	2448854.76	79.0	0.3	19	Thorburn
	1994 May 31/Jun 01	2449504.29	80.5	0.1	59	AAT/UCLES/CCD
	1994 Oct 24/25	2449649.89	80.2	0.1	57	AAT/UCLES/CCD
	1996 Sep 24	2450350.01	80.3	0.2	47	AAT/UCLES/CCD
CS 22892−052.....	1988–1990	...	13.1	0.3	...	McWilliam et al. (1995a)
	1994 Jun 20	2449524.27	13.1	0.2	34	AAT/UCLES/CCD
	1994 Jun 30	2449534.16	14.1	0.2	44	AAT/UCLES/CCD
	1994 Oct 24	2449649.97	13.5	0.2	52	AAT/UCLES/CCD

[a] Number of lines.
[b] Velocity determined, in part, with Fourier cross-correlation techniques.
[c] Image Photon Counting System.

While the results for CS 22892−052 are sparse, there is no evidence for velocity variations.

4.6. *Lithium*

A fairly strong case can be made that the *s*-process enhanced classes of Ba II giants, subgiant CH stars, Ba dwarfs, and the CH stars are Li depleted (see Smith & Lambert 1986, Lambert, Smith, & Heath 1993, and references therein). Insofar as LP 625−44 and LP 706−7 may be related to these objects it is interesting to consider their Li abundances. Fortunately, both of them were included in the Li abundance survey of Thorburn (1994, where LP 706−7 = G268−32), who reported N_c(Li) (= log N(Li)/N(H) + 12 at $T_{\rm eff}$ = 6300 K) values of less than 0.4 and 2.25, respectively. This should be compared with her determination of N_c(Li) = 2.32 for the Spite Plateau exhibited by halo main-sequence objects in the range $5600 < T_{\rm eff} < 6400$ K.

Taken at face value, Li is underabundant in LP 625−44: The results of Ryan & Deliyannis (1995, their Fig. 3) show that for our adopted $T_{\rm eff}$ = 5500 K, Li is depleted by 1 dex, while if one were to prefer the value $T_{\rm eff}$ = 5200 K adopted by Thorburn, the depletion is ∼0.5 dex. [We note that since $dN_c({\rm Li})/dT_{\rm eff} \sim 0.0008$ (Ryan et al. 1996a) these depletions are insensitive to the cited possible differences in $T_{\rm eff}$.]

The Li abundance of LP 706−7, in contrast, lies exactly on the Spite Plateau. Given the high temperatures one would associate with the production of the overabundances of C, N, and the *s*-process elements in this object this seems quite remarkable in view of the fragility of Li to destruction by (p, α) reactions at temperatures of a few million K. Li abundances in metal-poor, C-rich near–main-sequence objects may, however, be a poor indicator of their enrichment history, given published results for two others in the class—CS 22898−027 and CS 22958−042. For CS 22958−042 on the one hand, [Fe/H] = −3.3 and N_c(Li) < 1.99 (Thorburn 1994), indicating a small depletion, while CS 22898−027 on the other, has [Fe/H] = −2.0 and N_c(Li) = 2.52. (Thorburn & Beers 1992, and private communication) and is Li enhanced. Since the Spite Plateau has a dispersion of ∼0.10 dex (Thorburn 1994) these differences are quite significant.[5]

Where does this leave us in relation to the binary hypothesis for the production of the abundance anomalies of LP 625−44 and LP 706−7? Clearly, the radial-velocity data and the Li abundance for LP 625−44 are consistent with the model. The data for LP 706−7, in some contrast, are problematic: There is no clear evidence for radial-velocity variation and its Li abundance is normal. What is the chance that LP 706−7 is indeed a binary and we have been unlucky in not detecting the canonical signatures? If one assumes that it is related to the *s*-process–enriched objects noted above, a rough estimate of the probability is possible. Consider first the absence of clear radial-velocity variation: Monte Carlo analysis of the subgiant CH star data of McClure (1997) shows that the probability of making six observations at random over a 2300 day period[6] and measuring a variation no larger than 2.3 km s^{-1}, as defined by the data in Table 5, is ∼14%. Second, consider the normality of its Li abundance in comparison with data for the Ba dwarfs and the subgiant CH stars, both classes of which have near–main-sequence gravities. In all 15 such objects where the test has been made Li is depleted (Smith & Lambert 1986; Lambert et al. 1993, § 4). If one then places the probability of observing no Li depletion at less than 7%, it follows that the chance of finding the observed velocity data *and* no Li depletion in LP 706−7 is $\lesssim$1%.

It is difficult to understand the abundance patterns of LP 706−7 if it is not a binary system. For completeness, however, we recall two possibly relevant results from the literature. The first is the argument of Luck & Bond (1982) that the subgiant CH stars are post–helium core flash objects that have returned to the vicinity of the main sequence following extensive mixing during the core flash. The second is the discovery of Fugimoto, Iben, & Hollowell (1990) and Hollowell, Iben, & Fugimoto (1990) that at helium core flash zero heavy element low-mass stars experience strong mixing, which leads to large surface overabundances of C and N not unlike those seen in LP 706−7. The caveat here is that they do not find the effect in objects with even the smallest heavy element content. Further, no indication is given that the zero heavy element objects mix sufficiently for them to return to the vicinity of the main sequence. One wonders, nevertheless, if physical effects not fully accounted for in the models of low abundance stars might lead to extensive mixing at helium core flash and to stars such as LP 706−7.

4.7. *The Unique Case of the C, N, and r-process Enhanced Giant CS 22892−052*

The *r*-process enhancement of CS 22892−052 has been discussed by Sneden et al. (1994, 1996) and McWilliam et al. (1995a), who conclude that the *r*-process patterns result from supernova enrichment. Given, however, the large C and N enhancements of CS 22892−052 and the fact that large C/Fe and C/O are not normally associated with supernovae (see, e.g., Maeder 1992), this may offer only a partial explanation of the observed abundances.

We commented in § 4.2 on the supernova simulations of some 18–30 $M_\odot$ zero heavy element objects of Woosley & Weaver (1995), which produce little or no Fe and O, but large amounts of C. In all cases the remnant is a black hole. Perhaps such objects have caused the large [C/Fe] of CS 22892−052. The question that then arises is whether they could also produce the *r*-process enhancement. The results of Woosley et al. (1994) on neutron star production and the

[5] The origin of this large range in Li abundance lies somewhat outside the thrust of the present investigation. We refer the reader to Busso et al. (1995) and references therein for a comprehensive discussion of the question of Li enhancement/depletion in red giant branch and AGB stars, and possible abundance changes subsequent to putative binary mass transfer. It suffices here to note that while the majority of red giants appear to have Li depletions driven by envelope Li destruction in excess of those expected from envelope dilution as a star evolves from the main sequence into the red giant region, there appears to be a range in stellar mass (which Busso et al. (1995) identify as ∼5–6 $M_\odot$) in which Li *enhancement* results from the operation in the stellar envelope of the so-called Li transport mechanism involving the process $^3{\rm He}(\alpha,\gamma)^7{\rm Be}(e-,\nu)^7{\rm Li}$. In this mass range the final Li abundance depends on the relative efficiency of its production and destruction. While details of the resulting enhancements are not yet on a firm theoretical footing, the possibility thus exists that, depending on the binary configuration, the mass transfer mechanism could lead to both Li deficiencies and enhancements.

[6] For each of McClure's stars we started the clock at the first observation after JD 2445000, and of necessity we excluded HD 89948.

r-process during the explosion of a 20 $M_\odot$ object suggest not: The layers that provide the seeds for the *r*-process are by definition not available for expulsion in the black hole remnants of Woosley & Weaver (1995). Note, however, that the latter calculations do not include mass loss or rotation, which may modify the situation.

The canonical site for high C/O production is the AGB phase of intermediate-mass stars (Iben 1975), while Mathews & Cowan (1990) suggest that *r*-process enhancement may result from lower mass supernovae. One might speculate whether there exists a mass range near, say, 10 $M_\odot$ in which C dredge-up during AGB evolution is followed by *r*-process heavy element production in the subsequent supernova explosion.[7] The argument against this is that there is nothing really special about such objects, and one must then explain why CS 22892−052 is such a rare type of object, when 10 $M_\odot$, low-abundance stars were presumably not uncommon. (McWilliam et al. 1995a estimate an upper limit of 1 in 40 for the type of supernova that enriched CS 22892−052.)

Another putative site for the origin of the abundance patterns might be "hypernovae" of mass greater than $\sim 100\ M_\odot$. The models described, for example, by Woosley & Weaver (1982) and Woosley, Axelrod, & Weaver (1984) are surely suggestive of the production of C and N peculiarities. In their zero heavy element, 200–500 $M_\odot$ objects, convective dredge up of C-rich material occurs from the outer regions of a helium convective core. At 500 $M_\odot$ the CNO cycle produces large amounts of nitrogen from this carbon-rich material. For 200 $M_\odot$ objects, on the other hand, the final ejecta have O/C > 1. Inspection of an intermediate evolutionary stage for this object, however, shows that the 90 $M_\odot$ envelope outside the helium burning shell has C/O ∼ 10 (Woosley & Weaver 1982, Fig. 21). Given that these calculations take no cognizance of mass loss or pulsational instability, one wonders if more realistic modeling might result in the expulsion of C- and N-rich material into the interstellar medium. It would also be interesting to know if such objects were able to produce *r*-process elements, though one suspects that here too the layers that provide the seed nuclei might not be available for ejection in the standard models. Since "hypernovae" would presumably be uncommon, the rareness of CS 22892−052 type objects would not be unexpected. An additional attraction of such hypernovae is their possible contribution to the C overabundances in Figure 6 of § 4.2.

5. SUMMARY

Searches for very low metallicity halo stars have revealed that a significant number have very high overabundances of carbon, ∼1–2 dex. The low-resolution spectra of Beers et al. (1992) suggest that ∼14% of stars with [Fe/H] $\lesssim -2.5$ have stronger than normal *G* bands, but few high-resolution studies of such stars have been undertaken. To partially address this deficiency, we have observed and analyzed three metal-poor, CH-strong stars. Two—LP 625−44 and LP 706−7—are high proper motion stars of relatively low luminosity whose extreme CH strength was discovered following our earlier work (Ryan & Norris 1991a, 1991b), while the third is the BPS giant CS 22892−052, which has been discussed extensively by Sneden et al. (1994, 1996).

We have measured the abundances of 20 elements including C, N, and numerous heavier species up to Dy, using WIDTH6 analyses of single lines, and spectrum synthesis to study molecular (CH and CN), blended, or hyperfine–split features. The results indicate that [C/Fe] ∼ +2.0 in the two high proper motion stars, and ∼ +1.0 in the giant. All three have large overabundances of N and the heavy neutron capture elements, with [Ba/Fe] > +2.0 in the first two and +0.55 in the third. Whereas, however, we confirm the finding of Sneden et al. that the giant shows an *r*-process heavy element pattern, the less evolved stars exhibit *s*-process abundances, more in keeping with the characteristics of the *s*-process–enhanced subgiant CH stars of Luck & Bond (1982, 1991).

Noting the qualitative similarities between the abundance patterns of the two *s*-process stars of our study and certain other classes, in particular the CH giants, and the disk population subgiant CH stars and F str λ4077 stars, we investigated possible connections more closely. The popular mechanism for explaining CH stars involves mass transfer across a binary system containing an AGB star that has undergone envelope burning and third dredge-up leading to high C and *s*-process abundances in its outer layers. Some difficulties were encountered, however, in associating our stars with these objects. In the case of the near–main-sequence star LP 706−7, in particular, there is no evidence for radial-velocity variations and its Li abundance is quite normal for a halo dwarf. The probability of a subgiant CH star exhibiting no radial-velocity variation *and* normal Li is $\lesssim 1\%$, suggesting that the binary explanation may not apply to this object. We remind the reader of older suggestions that subgiant CH stars are extensively mixed, reevolving systems, which may retain merit and even be the explanation for our extremely C-rich halo systems, subject again to the requirement of preserving Li in LP 706−7.

The heavy-to-light *s*-process ratio, [hs/ls], is much higher in our metal-poor CH-strong stars than in the disk population, subgiant CH and F str λ4077 stars. The high neutron exposure per seed nucleus needed to achieve this points to a primary (^{13}C) rather than secondary (^{22}Ne) neutron source.

Finally, intrigued by the contrast between the *r*-process patterns in CS 22892−052 and the *s*-process patterns in the less evolved stars, we searched for supernova models that might provide large carbon and *r*-process element abundances without also producing intermediate mass elements. No obvious progenitor was identified: Those models capable of producing carbon prolifically were also those which did not eject the regions occupied by *r*-process seed nuclei.

We wish to thank G. W. Preston for constructive criticism of our discussion of the radial-velocity measurements. We are grateful to the Australian Time Allocation Committee for its continued support for our studies on the most metal-deficient stars and to the Director, R. D. Cannon, and staff of the Anglo-Australian Observatory for providing facilities for this study. J. E. N. and S. G. R. express their gratitude to the (Australian) Department of Industry, Science and Technology for provision of a grant from the

[7] A wilder speculation is a binary containing an intermediate-mass star that produces C during its AGB phase, loses mass to become a white dwarf, and later becomes a Type Ia deflagration supernova (during subsequent back mass transfer) causing *r*-process enrichment. The apparent absence of binarity of CS 22892−052, however, argues against the suggestion.

Bilateral Science and Technology Collaboration Program, which partially supported this work. J. E. N. gratefully acknowledges the hospitality of the Institute of Astronomy, University of Cambridge, during manuscript preparation; S. G. R. was supported by an Australian Research Council Postdoctoral Fellowship during part of the study; and T. C. B. acknowledges support from grants AST 90-1376, AST 92-22326, and INT 94-17547 awarded by the National Science Foundation.

REFERENCES

Barbuy, B., Cayrel, R., Spite, M., Beers, T. C., Spite, F., Nordstrom, B., & Nissen, P. E. 1997, A&A, 317, 63
Beers, T. C., Norris, J. E., & Ryan, S. G. 1997, in preparation
Beers, T. C., Preston, G. W., & Shectman, S. A. 1992, AJ, 103, 1987 (BPS)
Bell, R. A. 1983, private communication
Bell, R. A., Eriksson, K., Gustafsson, B., & Nordlund, Å., 1976, A&AS, 23, 37
Bond, H. E. 1992, Nature, 356, 474
Busso, M., Lambert, D. L., Beglio, L., Gallino, R., Raiteri, C. M., & Smith, V. V. 1995, ApJ, 446, 775
Carbon, D. F., Langer, G. E., Butler, D., Kraft, R. P., Suntzeff, N. B., Kemper, E., Trefzger, C. F., & Romanishin, W. 1982, ApJS, 49, 207
Cottrell, P. L., & Norris, J. 1978, ApJ, 221, 893
Cowan, J. J., Cameron, A. G. W., & Truran, J. W., Jr. 1982, ApJ, 252, 348
Cowley, C. R., & Downs, P. L. 1980, ApJ, 236, 648
Fugimoto, M. Y., Iben, I., Jr., & Hollowell, D. 1990, ApJ, 349, 580
Gass, H., Liebert, J., & Wehrse, R. 1988, A&A, 189, 194
Gibson, B. K. 1995, Ph.D. thesis, Univ. British Columbia
———. 1997, MNRAS, in press
Höhle, C., Hühnermann, H., & Wagner, H. 1982, Z. Phys. A, 304, 279
Hollowell, D., Iben, I., Jr., & Fugimoto, M. Y. 1990, ApJ, 351, 245
Iben, I., Jr. 1975, ApJ, 196, 525
Kraft, R. P., Suntzeff, N. B., Langer, G. E., Carbon, D. F., Trefzger, C. F., Friel, E., & Stone, R. P. S. 1982, PASP, 94, 55
Krebs, K., & Winkler, R. 1960, Z. Phys., 160, 320
Lambert, D. L. 1978, MNRAS, 182, 249
———. 1985, in Cool Stars with Excesses of Heavy Elements, ed. M. Jaschek & P. C. Keenan (Dordrecht: Reidel), 191
Lambert, D. L., Smith, V. V., & Heath, J. 1993, PASP, 105, 568
Langer, G. E., Kraft, R. P., Carbon, D. F., Friel, E., & Oke, J. B. 1986, PASP, 98, 473
Luck, R. E., & Bond, H. E. 1982, ApJ, 259, 792
———. 1991, ApJS, 77, 515
Maeder, A. 1992, A&A, 264, 105
Malaney, R. A. 1987, ApJ, 321, 832
Mathews, G. J., & Cowan, J. J. 1990, Nature, 345, 491
McClure, R. D. 1979, Mem. Soc. Astron. Italiana, 50, 15
———. 1997, preprint (astro-ph/9702034)
McClure, R. D., Fletcher, J. M., & Nemec, J. M. 1980, ApJ, 238, L35
McClure, R. D., & Woodsworth, A. W. 1990, ApJ, 352, 709
McWilliam, A., Preston, G. W., Sneden, C., & Searle, L. 1995a, AJ, 109, 2757
McWilliam, A., Preston, G. W., Sneden, C., & Shectman, S. A. 1995b, AJ, 109, 2736
Norris, J. E., & Da Costa, G. S. 1995, ApJ, 447, 680
Norris, J. E., Ryan, S. G., & Beers, T. C. 1996, ApJS, 107, 391
———. 1997, in preparation
North, P., Berthet, S., & Lanz, T. 1994, A&A, 281, 775
Rutten, R. J. 1978, Sol. Phys., 56, 237
Ryan, S. G. 1989, AJ, 98, 1693
Ryan, S. G., Beers, T. C., Deliyannis, C. P., & Thorburn, J. A. 1996a, ApJ, 458, 543
Ryan, S. G., & Deliyannis, C. P. 1995, ApJ, 453, 819
Ryan, S. G., & Norris, J. E. 1991a, AJ, 101, 1835
———. 1991b, AJ, 101, 1865
Ryan, S. G., Norris, J. E., & Beers, T. C. 1996b, ApJ, 471, 254
Ryan, S. G., Norris, J. E., & Bessell, M. S. 1991, AJ, 102, 303
Smith, V. V., Coleman, H., & Lambert, D. L. 1993, ApJ, 417, 287
Smith, V. V., & Lambert, D. L. 1986, ApJ, 303, 226
Sneden, C. 1973, ApJ, 184, 839
Sneden, C., McWilliam, A., Preston, G. P., Cowan, J. J., Burris, D. L., & Armosky, B. J. 1996, ApJ, 467, 819
Sneden, C., & Parthasarathy, M. 1983, ApJ, 267, 757
Sneden, C., Preston, G. W., McWilliam, A., & Searle, L. 1994, ApJ, 431, L27
Thorburn, J. A. 1994, ApJ, 421, 318
Thorburn, J. A., & Beers, T. C. 1992, BAAS, 24, 1278
Timmes, F. X., Woosley, S. E., & Weaver, T. A. 1995, ApJS, 98, 617
Tomkin, J., & Lambert, D. L. 1983, ApJ, 273, 722
Tomkin, J., Lemke, M., Lambert, D. L., & Sneden, C. 1992, AJ, 104, 1568
Tomkin, J., Woolf, V. M., Lambert, D. L., & Lemke, M. 1995, AJ, 109, 2204
Van Winckel, H., Waelkens, C., & Waters, L. B. F. M. 1995, A&A, 293, L25
Wheeler, J. C., Sneden, C., & Truran, J. W., Jr. 1989, ARA&A, 27, 279
White, H. E., & Eliason, A. Y. 1933, Phys. Rev., 44, 753
Woosley, S. E., Axelrod, T. S., & Weaver, T. A. 1984, in Stellar Nucleosynthesis, ed. C. Chiosi & A. Renzini (Dordrecht: Reidel), 263
Woosley, S. E., & Weaver, T. A. 1982, in Supernovae: A Survey of Current Research, ed. M. J. Rees & R. J. Stoneham (Dordrecht: Reidel), 79
———. 1995, ApJS, 101, 181
Woosley, S. E., Wilson, J. R., Mathews, G. J., Hoffman, R. D., & Meyer, B. S. 1994, ApJ, 433, 229